International Journal of Engineering and Advanced Technology (IJEAT)
ISSN: 2249-8958 (Online), Volume-4 Issue-3, February 2015

# Design Optimization of a 3 DOF Translational Parallel Manipulator

**S. Ramana Babu, V. Ramachandra Raju, K. Ramji**

***Abstract – This paper presents an optimal kinematic design of a 3PRC (prismatic-revolute-cylindrical) spatial translational parallel manipulator with inclined actuator arrangement by formulating a multi-objective optimization problem. Three performance criteria's namely Global Conditioning Index (GCI), Global stiffness Index (GSI) and Workspace volume are considered as the objective functions. A multi-objective evolutionary algorithm based on the control elitist non-dominated sorting genetic algorithm (CENSGA) is adopted to find the final approximation set.***

***Keywords: GCI, GSI, multi-objective genetic algorithm, Pareto front, GA, CENSGA***

## I. INTRODUCTION

In the recent years, there has been an increasing interest in the development of parallel manipulators. Early research on parallel manipulators concentrated primarily on 6-DOF parallel manipulators. Now a day's parallel manipulator s with fewer DOF (degree of freedom) has attained the focus of researchers due to their advantages such as simple in structure, reduction in manufacturing cost and easy to control when compared with higher DOF parallel manipulators. Kim and Tsai [1] presented a 3-DOF translational parallel manipulator called Cartesian parallel manipulators with three PRRR legs. Tsai and Joshi [2] enumerated the 3-DOF parallel manipulator for the design analysis and optimization. Kong and Gosselin [3] presented a method for the type synthesis of a 3-DOF parallel manipulator based on screw theory. Di Gregorio and Parenti Castle [4] presented the kinematic model and singularity analysis of a 3-DOF parallel manipulator with three RRPRR legs. Callegari and Tarantini [5] investigated the kinematic analysis of a 3-DOF translational mechanism with 3-RPC topology. The kinematic analysis of a new 3-DOF translational parallel manipulator with fixed actuators called 3PRC is investigated by the Li and Xu [6]. Stiffness is one of the most important performances of parallel manipulators, particularly for those which are used as machine tools, because higher stiffness manipulators can withstand for larger cutting forces without affecting the accuracy of the machining. The stiffness of a lower DOF tripod-based manipulator is studied by Huang et al [7] using the principle of virtual work.

**Manuscript published on 28 February 2015.**
***** Correspondence Author (s)
**S. Ramana Babu***, Department of Mechanical Engineering, Raghu Engineering College, Visakhapatnam, India.
**Dr. V. Ramachandra Raju**, Department of Mechanical Engineering, Jawaharlal Nehru Technological University, Kakinada, India.
**Dr. K. Ramji**, Department of Mechanical Engineering, Andhra University, Visakhapatnam, India.



The stiffness model of a 3-DOF CaPaMan parallel manipulator is established by Ceccarelli and Carbone [8] while considering the kinematic and static feature of the three legs. The stiffness analysis of a 3PRC translational parallel manipulator via screw theory is presented by Li and Xu [9]. Real world engineering design problems are characterized by many conflicting objectives .The presence of multiple objectives gives rise to a set of optimal solutions (Pareto optimal), rather than a single dedicated optimal solution. The designer can choose an appropriate solution from the Pareto front depends on his requirements and priority given to a specific objective function. In classical optimization the multi objective problem is to be converted into a single objective problem by emphasizing one specific Pareto optimal solution at a time. Because of their population-based nature the evolutionary algorithms are able to find multiple Pareto optimal solutions in a single run. It is necessary to find the appropriate geometrical parameters for any parallel manipulator for the improved characteristics of the robot workspace for the enhanced applications. Optimization methodologies have long been applied to mechanism design and a number of different optimization criteria for robot manipulators have been proposed. Liu et al [10] have introduced an approach to do optimum design of 3-DOF spherical parallel manipulators in order to optimize the performance indices GCI and GSI. Study of parallel manipulators with the optimization criteria as the manipulability of the manipulator was done by Alice and Shirinzadeh [11]. Rao and Rao [12] have performed the dimensional synthesis of a 3-RPS parallel manipulator using a hybrid optimization method called GA-simplex method. Lara-Molina et al [13] performed the optimal design of a spatial Stewart-Gough platform based on multi-objective optimization; the objective functions are Global Condition Index, Global Payload Index (GPI) and Global Gradient Index (GGI) using multi-objective Evolutionary Algorithm (MOEA). Lopes and Solteiro Pires [14] formulated an optimization problem in order to minimize power consumption and maximize the stiffness of the manipulator using a multi-objective genetic algorithm in order to find the work piece location in a machining Robotic cell. Kelaiaia et al [15] presented an approach for dimensional synthesis for parallel manipulators in order to maximize the performance (Workspace, stiffness, kinematic, dynamic performance) using the strength Pareto evolutionary algorithm-II (SPEA-II). A parallel manipulator that is optimized for total workspace will result in a manipulator with undesirable kinematic and static characteristics such as poor dexterity and more compliance.

For many applications, the manipulator is preferred to be designed with emphasis on Global conditioning index (GCI) and Global stiffness index (GSI) along with the workspace volume. Even though the kinematic and static analysis of 3PRC parallel manipulators is investigated by the earlier researchers, design of manipulator for optimal performance is not performed. In the present work the design optimization of a 3PRC manipulator with adjustable actuator layout angle is performed, by considering the three performance indices GCI, GSI and Workspace volume and optimal solutions are found through the controlled elitist non-dominated sorting genetic algorithm. The organization of the paper is as follows. Section 2 briefs the geometric description of the 3PRC parallel manipulator. The mobility analysis and jacobian matrix derivation are described in section 3. In section 4 workspace analysis is presented, in section 5 stiffness analysis is presented.

Performance indices and its significance are explained in section 6.After that a multi-objective optimization is described in section 7, the results are discussed in section 8.Finally the paper concludes in section9.

## II. DESCRIPTION OF THE MECHANISM OF THE MANIPULATOR

The CAD model of a 3-PRC mechanism is shown in Fig.1. It consists of a mobile platform, fixed platform and three limbs that connecting the fixed and moving platforms.

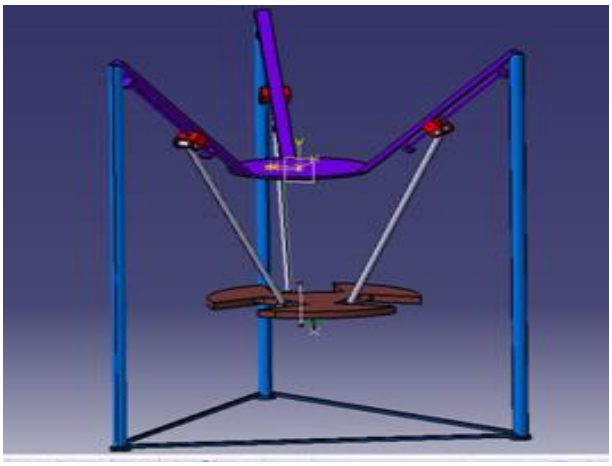

**Fig. 1 CAD model of 3PRC manipulator**

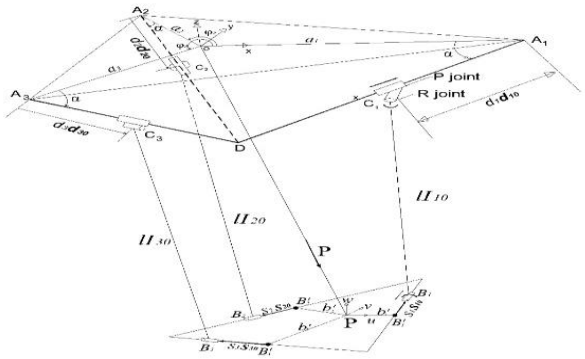


**Fig. 2 Schematic representation of 3PRC mechanism**

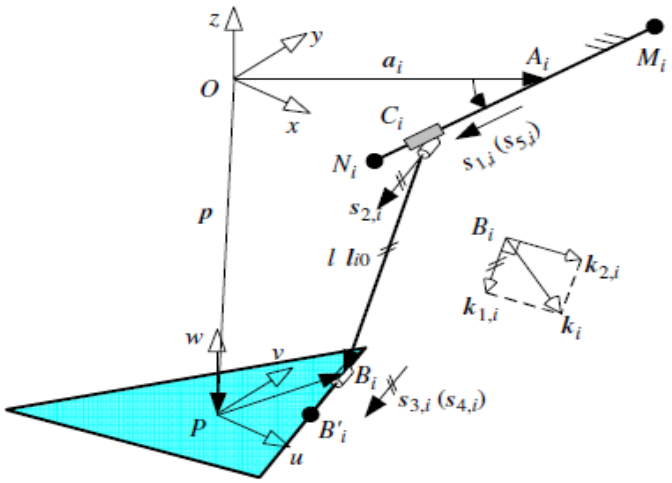


**Fig. 3 Representation of screws for a leg**

Each limb consists of a prismatic joint (P), a revolute joint, and a cylindrical joint (C) in sequence, where P joint is connected to the fixed base. The vector representation of the mechanism is shown in Fig.2. A fixed frame $O\{x, y, z\}$ is attached to the centre point of the fixed base, and a moving frame $P\{u, v, w\}$ is attached at the centered point, . The $i\,th$ limb $C_iB_i$ $(i = 1,2,3)$ has a length of $l$ is connected to the mobile platform at $B_i$ which is a point on the axis of the $ith$ C joint, where as the three points$B_i'$, for $i = 1,2,3$ lie on circle of radius $b$. The axis of P joint is perpendicular to the axes of R and C joints within the $ith$ limb. Angle $\alpha$ is measured from the fixed base to rails $A_iD$ defined as the actuator layout angle. In order to achieve the symmetric workspace both $\Delta A_1A_2A_3$ and $\Delta B_1B_2B_3$ are considered as equilateral triangles. The unit vectors $\mathbf{l}_{i0}$ , $\mathbf{d}_{i0}$ ,$\mathbf{s}_{i0}$ are directing along $C_iB_i$ ,$A_iD$, $B_iB_i'$ respectively, where as the linear displacement of $ith$ P joint is $d_i$ and $s_i$ for the $ith$ C joint. Referring to Fig.2 the vector loop equation for the $ith$ limb can be expressed as


Published By:
Blue Eyes Intelligence Engineering
and Sciences Publication (BEIESP)

$$l\mathbf{I}_{i0} = \mathbf{P} + \mathbf{b}_i^{'} + s_i\boldsymbol{s_{i0}} - \mathbf{a}_i - d_i\mathbf{d}_{i0} \quad (1)$$

According to this the inverse kinematic solution can be derived (see [6] for more details), that are used to determine the reachable workspace of the 3-PRC parallel manipulator, on dot multiplying the eq. (1) with itself gives as

$$d_i = \mathbf{d}_{i0}^T\ \mathbf{e}_i - \sqrt{(\mathbf{d}_{i0}^T\ \mathbf{e}_i)^2 - \mathbf{e}_i^T\ \mathbf{e}_i + l^2} \quad (2)$$

Where $\mathbf{e}_i = \mathbf{P} + \mathbf{b}_i^{'} + s_i\boldsymbol{s_{i0}} - \mathbf{a}_i$ for $i = 1,2,3$

## III. MOBILITY ANALYSIS AND JACOBIAN MATRIX

The motion of the mobile platform can be expressed by a instantaneous twist $\$_p$ as a linear combination of the four instantaneous twists,

$$\$_p = \dot{d}_i\hat{\$}_{1,i} + \dot{\theta}_{2,i}\,\hat{\$}_{2,i} + \dot{\theta}_{3,i}\,\hat{\$}_{3,I} + \dot{s}_I\,\hat{\$}_{4,I} \quad (3)$$

for $i = 1,2,3$ where $\dot{\theta}_{j,I}$ is the intensity and $\hat{\$}_{j,I}$ denotes a unit screw associated with the $jth$ joint of the $ith$ limb with respect to the instantaneous reference frame $\boldsymbol{P}$ as shown in Fig.3 . The screws that are reciprocal to all the joint screws of one limb of the manipulator form a 2-system. There are two infinite-pitch reciprocal screws (constraint couples) are identified for each limb, there are total six wrench screws for the manipulator, out of the six only three are linearly independent, so forms 3-order wrench system. In order to eliminate the over constraints of the mechanism, add a R joint with the common axis of the P joint in the $ith$ limb. The instantaneous twists twist $\$_p$of the mobile platform can be expressed as a linear combination of five instantaneous twists as

$$\$_p = \dot{d}_i\hat{\$}_{1,i} + \dot{\theta}_{2,i}\,\hat{\$}_{2,i} + \dot{\theta}_{3,i}\,\hat{\$}_{3,I} + \dot{s}_I\,\hat{\$}_{4,I} + \dot{\theta}_{5,i}\,\hat{\$}_{5,i} \quad i = 1,2,3 \quad (4)$$

The screws that are reciprocal to all the joint screws of limb form a 1-system, the reciprocal screw of the $ith$ limb can be identified as an infinite-pitch wrench screw as $\hat{\$}_{c,I} = [0 \quad \mathbf{k}_i]^T$ , where $\mathbf{k}_i$ is a unit vector defined by

$$\mathbf{k}_i = \frac{s_{2,i} \times s_{5,i}}{\| s_{2,i} \times s_{5,i} \|} \quad (5)$$

Taking the reciprocal product on both sides of eq.(4) with $\hat{\$}_{c,I}$ and it can be expressed in matrix form

$$\mathbf{J}_c\$_p = 0 \quad (6)$$

Where

$$\mathbf{J}_c = \begin{bmatrix} \mathrm{k}_1^{\mathrm{T}} & 0^{\mathrm{T}} \\ \mathrm{k}_2^{\mathrm{T}} & 0^{\mathrm{T}} \\ \mathrm{k}_2^{\mathrm{T}} & 0^{\mathrm{T}} \end{bmatrix}$$

Is called the jacobian of constraints [9], [16]. Each row in $\mathbf{J}_c$ denotes an unit wrench of constraints imposed by the joints of a limb, the combination of which constrains the mobile platform to a 3-DOF motion, the unique solution to eq.(6) is $\omega = 0$. Secondly, with the actuators locked the reciprocal screw of each limb form a 2-system. The screw reciprocal to all the passive joint screws of the $ith$ limb can be identified as a zero-pitch screw along the direction of the $ith$ leg as

$$\hat{\$}_{a,i} = \begin{bmatrix} \mathbf{I}_{i0} \\ \mathbf{b}_i \times \mathbf{I}_{i0} \end{bmatrix} \quad (7)$$

Taking the reciprocal product on both sides of eq.(4) with $\hat{\$}_{a,i}$ and expressed in the matrix form as

$$\mathbf{J}_a\$_p = \dot{\mathbf{q}} \quad (8)$$

Where $\dot{\mathbf{q}} = [\dot{d}_1 \quad \dot{d}_2 \quad \dot{d}_3]^{\mathrm{T}}$ denotes the actuated joint rates and

$$\mathbf{J}_a = \begin{bmatrix} \frac{(\mathbf{b}_1 \times \mathbf{I}_{10})^{\mathrm{T}}}{\mathbf{I}_{10}^{\mathrm{T}} s_{1,1}} & \frac{\mathbf{I}_{10}^{\mathrm{T}}}{\mathbf{I}_{10}^{\mathrm{T}} s_{1,1}} \\ \frac{(\mathbf{b}_2 \times \mathbf{I}_{20})^{\mathrm{T}}}{\mathbf{I}_{20}^{\mathrm{T}} s_{1,2}} & \frac{\mathbf{I}_{10}^{\mathrm{T}}}{\mathbf{I}_{20}^{\mathrm{T}} s_{1,2}} \\ \frac{(\mathbf{b}_3 \times \mathbf{I}_{30})^{\mathrm{T}}}{\mathbf{I}_{30}^{\mathrm{T}} s_{1,3}} & \frac{\mathbf{I}_{10}^{\mathrm{T}}}{\mathbf{I}_{30}^{\mathrm{T}} s_{1,3}} \end{bmatrix}$$

is called the jacobian of actuations.

## IV. WORKSPACE ANALYSIS

The workspace of a parallel manipulator is one of the most important criteria which reflect its working capacity. So it is necessary to analyze shape and size of the workspace volume for enhancing the applications of parallel manipulators. While designing a practical manipulator the physical constraints interns of the range of parasitic motions of the end-effecter and limits of the linear actuators, leg interferences and limitations on the passive joints are to be considered, Gosselin [17], Merlet [18] presented an algorithm enabling to compute the possible rotation of the end-effecter around a fixed point. The workspace volume is evaluated by the following formula as

$$V = \sum_{Z_i = Z_{\min}}^{Z_{\max}} \sum_{\theta_z = 0}^{2\pi} \left(\frac{1}{2}\rho_i^2 \Delta\theta_z \Delta z\right) \quad (9)$$

In the above equation $\rho_i$ is polar ray, $\Delta\theta_z$ angle of increment when rotating about Z axis and $\Delta z$ is small increment along the Z axis.

## V. STIFFNESS MATRIX DETERMINATION

The external wrench can be expressed as $\mathbf{w} = [\mathbf{f}^{\mathrm{T}} \quad \mathbf{m}^{\mathrm{T}}]^{\mathrm{T}}$ in plucker ray coordinate, where $\mathbf{f}$ and $\mathbf{m}$ denotes a force and torques exerted on mobile platform. The external wrench is balanced by the reaction forces/torques exerted by the actuators and constraints as

$$\mathbf{w} = \mathrm{J}_a^{\mathrm{T}}\,\boldsymbol{\tau}_a + \mathbf{J}_c^{\mathrm{T}}\,\boldsymbol{\tau}_c \quad (10)$$

Where the reaction forces/torques can be expressed as

$$\boldsymbol{\tau}_a = \boldsymbol{\chi}_a \Delta\mathbf{q}_a \quad (11)$$


Published By:
Blue Eyes Intelligence Engineering
and Sciences Publication (BEIESP)

$$\boldsymbol{\tau}_c = \boldsymbol{\chi}_c \Delta \mathbf{q}_c \quad (12)$$

Where $\Delta \mathbf{q}_a$ and $\Delta \mathbf{q}_c$ denotes the displacements of actuations and constraints, $\boldsymbol{\chi}_a$ and $\boldsymbol{\chi}_c$ are the diagonal matrices of stiffness coefficients of actuations, constraints respectively. Let $\Delta \mathbf{x} = [\Delta x \quad \Delta y \quad \Delta z]^{\mathrm{T}}$ and $\Delta \boldsymbol{\theta} = [\Delta \theta_x \quad \Delta \theta_y \quad \Delta \theta_z]^{\mathrm{T}}$ be the infinitesimal displacements of translation and rotation of the mobile platform with respect to the reference frame, applying the principle of virtual work gives as

$$\mathbf{w}^{\mathrm{T}} \Delta \mathbf{X} = \boldsymbol{\tau}_a^{\mathrm{T}} \Delta \mathbf{q}_a + \boldsymbol{\tau}_c^{\mathrm{T}} \Delta \mathbf{q}_c \quad (13)$$

Where $\Delta \mathbf{X} = [\Delta \mathbf{x}^{\mathrm{T}} \quad \Delta \theta^{\mathrm{T}}]^{\mathrm{T}}$ denotes the mobile platform twist deformation. From the eqs.(10)−(13) can express as

$$\mathbf{w} = \mathbf{K} \Delta \mathbf{X} \quad (14)$$

Where $\mathbf{K} = \mathbf{J}^{\mathrm{T}} \boldsymbol{\chi} \mathbf{J}$ is the overall stiffness matrix, $\boldsymbol{\chi} = diag[\boldsymbol{\chi}_a \quad \boldsymbol{\chi}_c]$ , $\mathbf{J} = \begin{bmatrix} \mathbf{J}_a \\ \mathbf{J}_c \end{bmatrix}$

## VI. PERFORMANCE MEASURES

### 6.1 Global condition Index

Dexterity is an important issue for design, trajectory planning, and control of manipulators. The dexterity of a manipulator can be the ability of the manipulator to arbitrarily change its position and orientation, dexterity is measured in terms of the jacobian matrix. The condition number of a jacobian matrix is expressed as

$$k = \|\mathbf{J_a}\| \, \|\mathbf{J}_a^{-1}\| \quad (15)$$

Where $\mathbf{J}_a$ is the jacobian matrix which is described in Eq.(8). Condition number signifies the error amplification factor between the joint rate errors to task space errors. The condition number depends on the manipulator configuration. The condition number varies from one at isotropic configurations to infinity at singular configurations so this is also defined as the measure of degree of ill-conditioning of the jacobian matrix. The reciprocal of the condition number $(1/k)$ is referred to as the conditioning index which is the local measure of performance of the manipulator at a particular pose of the end-effecter within in the workspace. In order to evaluate the global behavior of a manipulator over the workspace, the GCI is expressed as

$$\text{GCI} = \frac{\int_W (\frac{1}{k}) dW}{\int_W dW} \quad (16)$$

Where $W$ is the workspace, $k$ is the condition number.

### 6.2 Global Stiffness Index

If an external wrench exerts on the moving platform, there is a deformation along different directions which can regarded as being distributed on an ellipsoid sphere with the lengths of major axis and minor axis being the maximum and minimum value of the deflection, respectively. This deformation is dependent on the manipulator's stiffness and on the external wrench. The manipulator stiffness affects the position accuracy of the device, so stiffness is considered as an important performance index. The GSI is the inverse of the condition number of the stiffness matrix integrated over the reachable workspace by the volume of the workspace, which can be expressed mathematically as

$$\text{GSI} = \frac{\int_W (\frac{1}{k_c}) dW}{\int_W dW} \quad (17)$$

Where $k_c = \|\mathbf{K}\| \, \|\mathbf{K}^{-1}\|$ , the global stiffness matrix $\mathbf{K}$ is described in Eq. (14).

## VII. MULTI-OBJECTIVE OPTIMIZATION

A multi-objective optimization problem has a number of objective functions usually conflicting with each other are to be minimized or maximized, a general form of the multi-objective minimization problem is expressed as

$$\text{Minimize } F(x) = (f_1(x), f_2(x), \ldots, f_i(x)) \quad (i=1, 2 \ldots M)$$

$$\text{Subjected to } g_j(x) \le 0 \qquad (j=1, 2 \ldots J)$$

$$h_k(x) = 0 \ (k=1, 2 \ldots K) \quad (18)$$

A solution x is a vector of n decision variables $x = (x_1, x_2 \ldots x_n)$. The desired solution is in the form of trade off or compromise among the solutions that would optimize all objectives simultaneously. The optimal trade off solutions among the objectives is called as Pareto optimal solutions. A curve formed by joining all these solutions is known as Pareto-optimal front which is the set of non-dominated solutions. The non-dominated solutions are those that are not dominated by any member of that set.

### 7.1. Controlled Elitist Non-dominated Sorting Genetic Algorithm

The preferred multi objective evolutionary algorithm to solve this optimization problem is the controlled elitist non-dominated sorting genetic algorithm (CENSGA), a variant of NSGA- II for controlling the extent of the elite members of the population and to maintain the diversity of the population for convergence to a final approximation set. In this algorithm the combined population $R_t = P_t \cup Q_t$ of size 2N is formed, and then $R_t$ is sorted according to non-domination. Since all previous and current population members are included in $R_t$ so elitism is ensured. Let us assume that the number of non dominated fronts formed in the combined population is $k$. The maximum number of individuals allowed in the $i_{th}$ front of a new population $P_{t+1}$ for the $(t+1)$ generation is given by

$$N_i = N \frac{1-r}{1-r^k} r^{i-1} \quad (19)$$


Published By:
Blue Eyes Intelligence Engineering
and Sciences Publication (BEIESP)

Where $r$ is the reduction rate, a user defined parameter
Thus the main concept of CENSGA is to forcibly allow at least certain number of solutions from each non-dominated fronts of $R_t$ to co-exist in the new population $P_{t+1}$ of size N. The new population $P_{t+1}$ is now used for selection, crossover and mutation to create a population $Q_{t+1}$ of size N, and then $R_{t+1}$ is formed by combining $P_{t+1}$ and$Q_{t+1}$ for the non-dominated sorting. The selection of specified number of solutions from each front is achieved by crowded tournament selection. The concept of CENSGA is almost same as that of NSGA-II except the controlled elite preserving mechanism; the new population obtained in CENSGA will be more diverse than that obtained in NSGA-II.

## VIII. RESULTS AND DISCUSIONS

### 8.1 Workspace simulation

Symmetric architectures are commonly considered in literature, a 3PRC manipulator in which both fixed and moving platforms are equilateral triangles with $OA_i = a$ =0.6m and $PB_i = b = 0.3$ m has been considered as an example. The linear movement of actuators is within ±0.2m, the length $l$ for each leg is 0.7 m, and linear movement of cylindrical joint is limited within ±0.1m, actuator layout angle $\alpha = 45^0$ is considered. The reachable workspace volume of 3PRC manipulator is shown in Fig.4, which is computed using numerical search method by solving the inverse kinematic equations through Mat lab programming. The workspace volume is continuous and there are no vertical gaps along the $Z$-coordinate, the workspace volume appears like a hexagonal prism for the middle portions, but like a triangular prism for the top and bottom portions. The cross sectional workspace at various sections is shown in Fig.5. The work envelop of 3PRC parallel manipulator appeared as a hexagonal shell is shown in Fig.6.

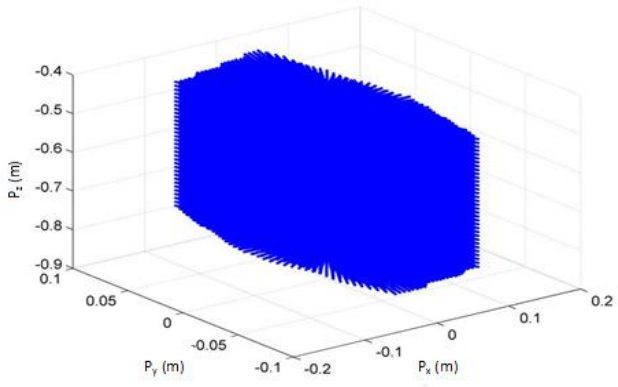


**Fig. 4 Workspace Volume of 3PRC manipulator**

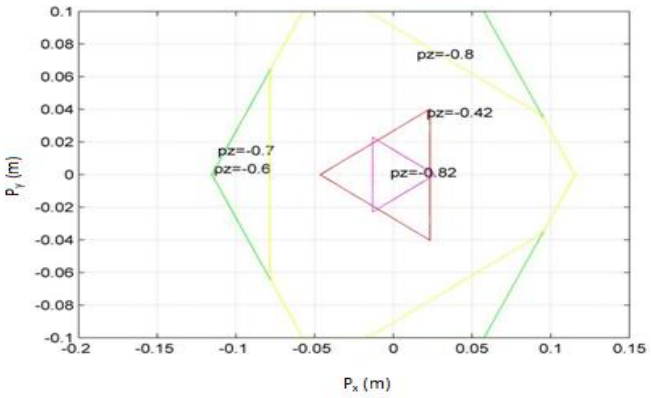


**Fig. 5 Cross sectional workspace**

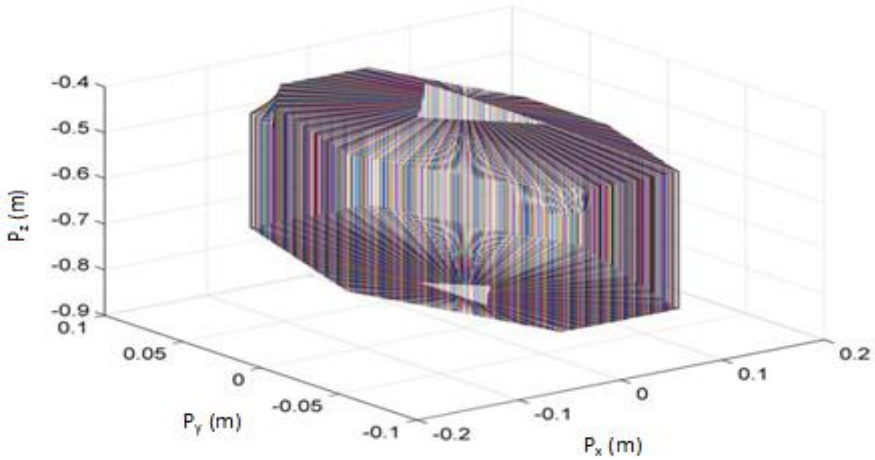


**Fig. 6 Work envelope of 3PRC manipulator**

### 8.2 Dexterity Measures of 3PRC manipulator

The condition index (CI) of the manipulator is dependent on the end effecter‘s pose; it varies from one point to another point within the workspace so it is a local measure of performance. In order to measure the global performance we have considered two global performance indices GCI and GSI. The variation of GCI, GSI with actuator’s layout angle is shown in Fig.7, Fig.8 respectively. It is observed that GCI is continuously decreasing with increase of actuator layout angle, it registered its maximum at $\alpha$ =$0^0$; whereas GSI has its maximum at $\alpha$ =$12^0$ afterwards a decreasing trend is observed.


Published By:
Blue Eyes Intelligence Engineering
and Sciences Publication (BEIESP)

The numerical results of workspace volume of 3PRC manipulator with changing actuator layout angle is shown in Fig.9, it can be observed that the workspace volume has attained its maximum at $\alpha$ =60$^0$, after that a continuous decreasing trend is observed. It is necessary to choose an appropriate actuator layout angle so as to achieve an equal compromise between GCI and GSI and workspace volume for enhanced applications of 3PRC manipulator.

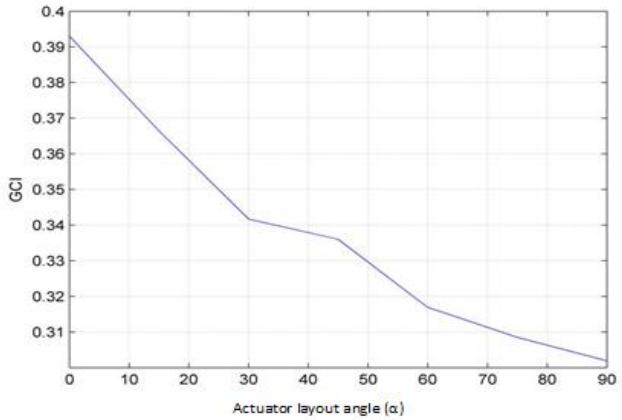


**Fig. 7 GCI versus actuator layout angle**

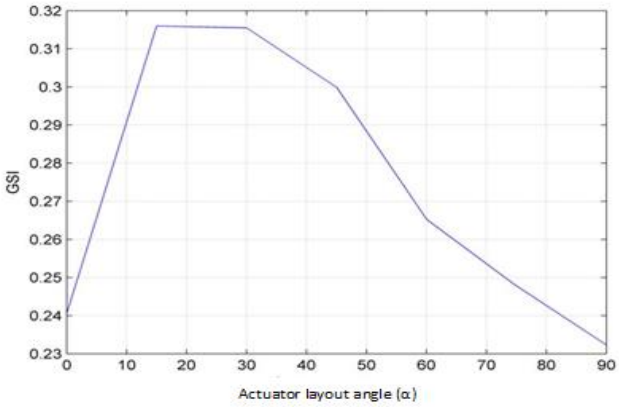


**Fig. 8 GSI versus actuator layout angle**

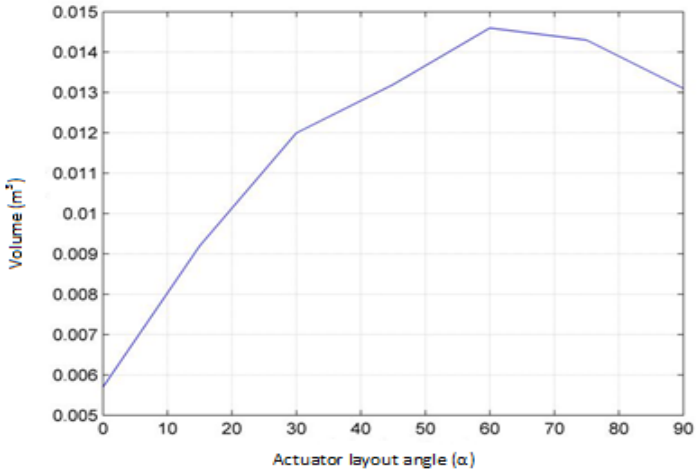


**Fig. 9 Workspace Volume versus actuator layout angle**

### 8.3 Simulation of GA

There are seven GA simulations are performed using the Mat lab optimization toolbox. The first three simulations are performed as a single objective optimization problem to maximize the GCI, GSI and workspace volume separately. As a part of multi objective optimization firstly considered GCI, workspace volume are objectives, secondly GSI and workspace volume and then GCI, GSI for the next simulation. A three-objective optimization problem is solved while considering the GCI, GSI and Workspace volume simultaneously.

#### 8.3.1 Single-Objective GA

The optimal design vector $x = [a \quad b \quad l \quad \alpha]$ for the maximum GCI is to be found as a single objective optimization problem in which the design parameters are allowed to change in the range $a \in [0.50,0.70], b \in [0.20, 0.40], l \in [0.6,0.75], \alpha\epsilon\ [10^0, 90^0]$, $d_{i\min} \le d_i \le d_{i\max}$ = ±0.2 m and, and linear movement of cylindrical joint is limited within ±0.1m. After some preliminary runs, have to set the GA parameters for simulation of the single objective GA are given in Table.1, the GCI is evaluated and the results are shown in Fig.10. The maximum GCI of 0.816 is attained for the design vector $x =$ [0.700 0.2013 0.6010 83.64$^0$]. The global stiffness index (GSI) is maximized as a second single objective problem, subjected to the same constraint bounds mentioned above. The evolution of GSI as a function of generations is shown in Fig.11; the maximum GSI of 0.6209 corresponding to the optimal design vector $x =$ [0.699 0.202 0.617 11.04$^0$] is attained. In the third GA simulation workspace volume is maximized for the same set of bound constraints given above, the evolution of workspace volume as a function of generations is shown in Fig.12. The maximum workspace volume of 0.0152 m$^3$ for the design vector $x =$ [0.6708 0.2597 0.7455 62.15$^0$] is obtained. The design vector is not same in all the three single objective simulation runs for the evolution of maximum fitness values, so it is observed that there is a conflicting among the objectives for their optimal values. From the above results it is observed that GSI is greatly influenced by the actuator layout angle ( $\alpha$) and the workspace volume is mostly influenced by the size of the fixed and moving platforms.


*Published By:*
*Blue Eyes Intelligence Engineering and Sciences Publication (BEIESP)*

**Table 1.Simple GA Parameters**

| Parameter | setting |
|---|---|
| Population size | 60 |
| Maximum generations | 100 |
| Encoding type | Real |
| Selection strategy | Stochastic sampling |
| Crossover type | Scattered |
| Mutation type | Adaptive |

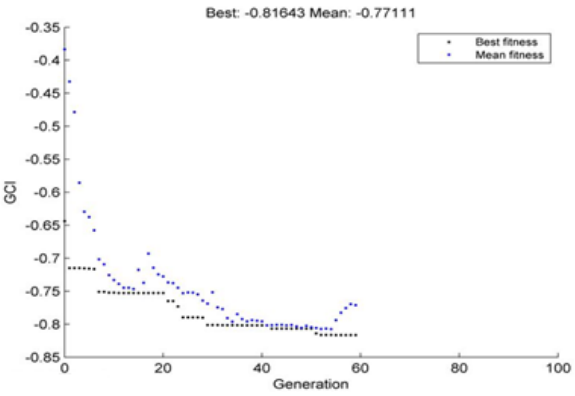


**Fig. 10 convergence of GCI**

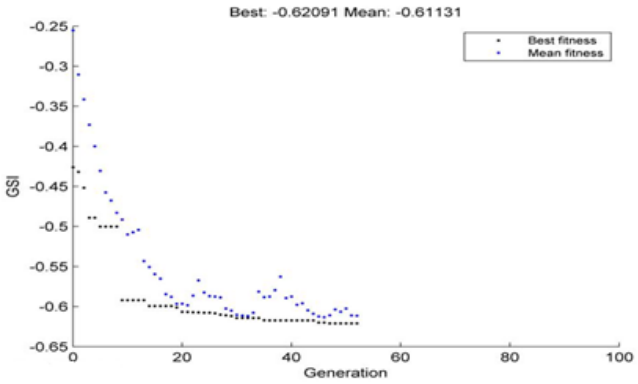


**Fig. 11 convergence of GSI**

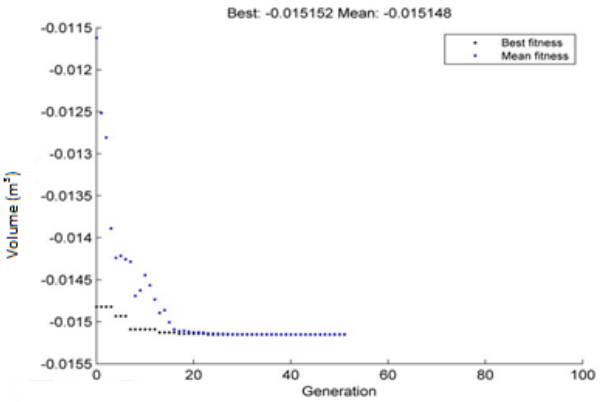


**Fig. 12 convergence of Workspace Volume**

### 8.3.2 Simulation of Multi-objective optimization

This section develops several experiments with three objectives GCI, GSI, workspace volume. After some preliminary simulations, have set simulation parameters to run the CENSGA are given in Table.2. Firstly a two objective optimization using two objectives at a time (GCI vs. volume, GSI vs. volume, GCI vs. GSI) optimization is performed; the corresponding final approximation sets are shown in Fig.13, 14&15 respectively. The final approximation front for GCI vs. volume is achieved by varying the design parameters in a specific ranges, which are observed for $a = [0.6890\ 0.6919]$, $b = [0.211\ 0.292]$ , $l = [0.641\ 0.745]$, $\propto = [20.22^0\ 56.05^0]$. The design parameters for final approximation front for GSI vs. volume varies as for $= [0.682\ 0.699]$ , $b = [0.206\ 0.280]$ ,$l = [0.662\ 0.743]$ , $\propto = [16.85^0\ 74.74^0]$. The design parameters for final approximation front of GCI vs. GSI varies as for $a = [0.690\ 0.691]$ , $= [0.224\ 0.227]$ ,$l = [0.613\ 0.616]$ , $\propto = [17.35^0\ 62.73^0]$.

In the next simulation of multiobjective optimization, three objective functions GCI, GSI and workspace volume are optimized simultaneously for the same CENSGA parameters that are set for a two objective optimization. The three dimensional final approximation set in criterion space is shown in Fig.16, some non-dominated solutions of the final approximation set corresponding to the three objectives (GCI, GSI and workspace volume) are given in Table.3. The final approximation front is obtained by varying the design parameters in a specific range, which are for $a = [0.676\ 0.699]$ , $b = [0.202\ 0.223]$, $l = [0.663\ 0.750]$, $\propto = [20.40^0\ 32.79^0]$.


Published By:
Blue Eyes Intelligence Engineering
and Sciences Publication (BEIESP)

While in the three objective optimization the functional variation of GCI, workspace volume in a two dimensional approximation set is shown in Fig.17; in which it is observed that GCI and workspace volume are quarrelsome each other for their optimal values. The ideal solution would be maximizes both the functions so an intermediate solution is to be chosen depending on the designer's choice. The final approximation set for GSI, workspace volume in three objective optimization is shown in Fig.18, in which it is observed that they quarrelsome each other for their optimal solution. The final approximation set for GCI and GSI is also shown in Fig.19, it is observed that both can follow a similar approach, one is increasing the other one is also increasing.

**Table 2.CENSGA Algorithm Parameters**

| Parameter | setting |
|---|---|
| Population size | 70 |
| Maximum generations | 100 |
| Encoding type | Real |
| Selection strategy | Tournament |
| Tournament size | 2 |
| Crossover type | Intermediate |
| Crossover ratio | 0.9 |
| Mutation type | Adaptive |
| Reduction factor r | 0.6 |

**Table 3. Pareto optimal solutions three objective optimization**

| $x = [a\ \ b\ \ l\ \ \alpha]$ | GCI | GSI | Workspace Volume ($m^3$) |
|---|---|---|---|
| 0.694 0.202 0.7480 $21.83^0$ | 0.513 | 0.629 | 0.0039 |
| 0.678 0.213 0.7474 $29.83^0$ | 0.456 | 0.572 | 0.0045 |
| 0.689 0.202 0.7484 $24.19^0$ | 0.493 | 0.611 | 0.0042 |
| 0.695 0.205 0.6633 $20.40^0$ | 0.550 | 0.660 | 0.0028 |
| 0.699 0.202 0.6737 $20.44^0$ | 0.541 | 0.654 | 0.0028 |
| 0.676 0.207 0.7480 $30.58^0$ | 0.455 | 0.575 | 0.0045 |
| 0.697 0.204 0.7500 $21.90^0$ | 0.513 | 0.630 | 0.0039 |
| 0.687 0.202 0.7458 $32.07^0$ | 0.458 | 0.594 | 0.0044 |
| 0.692 0.211 0.7486 $26.61^0$ | 0.477 | 0.597 | 0.0044 |

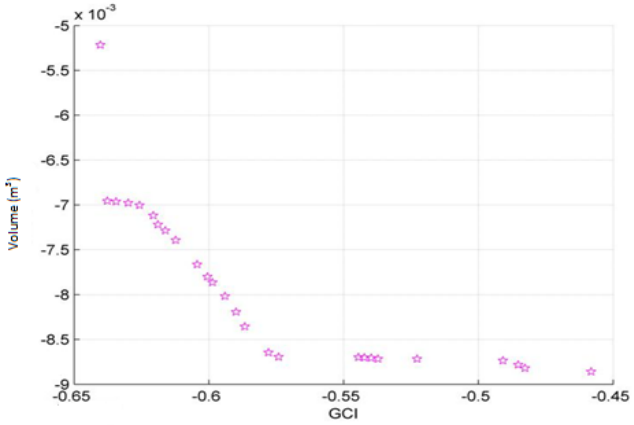


**Fig. 13 Pareto front GCIVs volume**

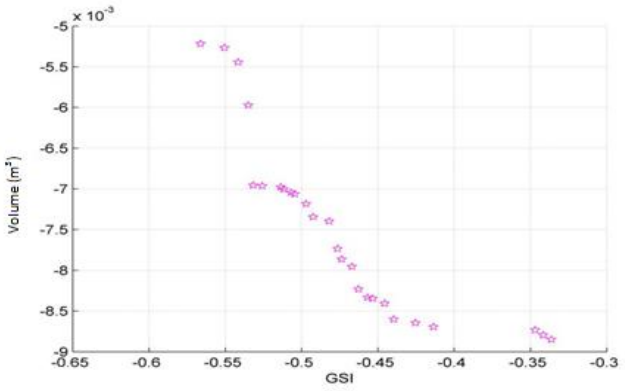


**Fig. 14 Pareto front GSI Vs volume**

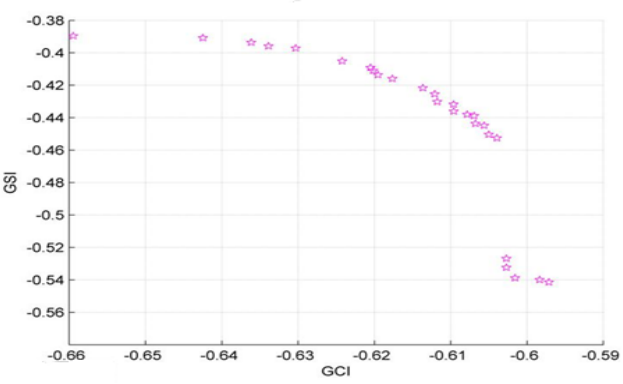


**Fig. 15 Pareto front GCI vs. GSI**

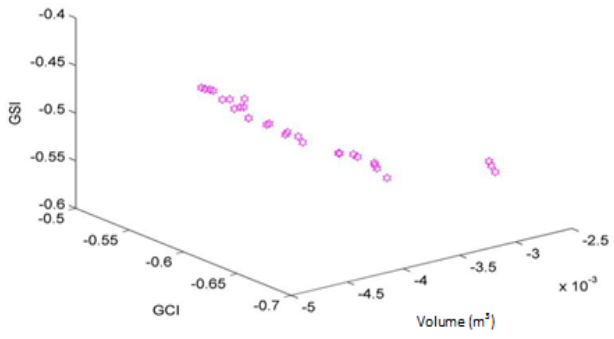


**Fig. 16 Pareto front for GCI vs. GSI vs. volume**


Published By:
Blue Eyes Intelligence Engineering
and Sciences Publication (BEIESP)

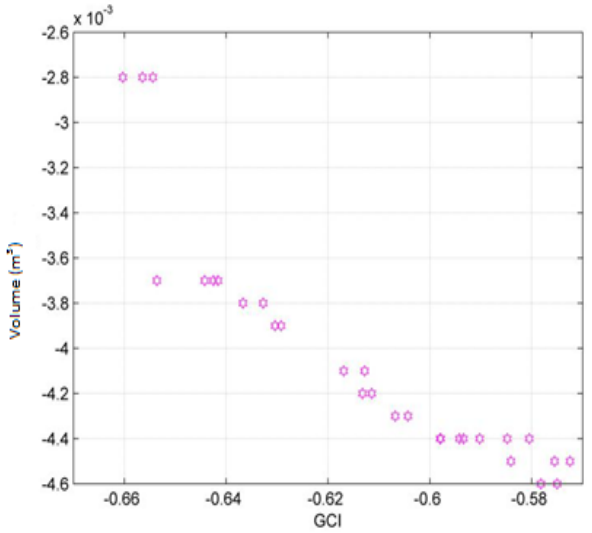


Fig. 17 Pareto optimal front for GCI vs. volume

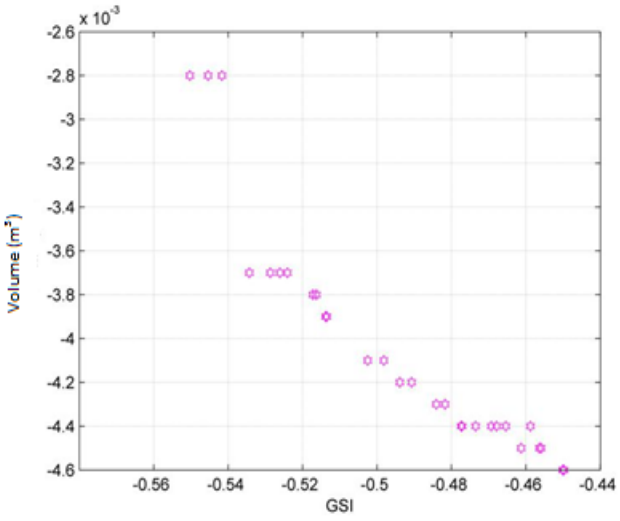


Fig. 18 Pareto optimal front for GSI vs. volume

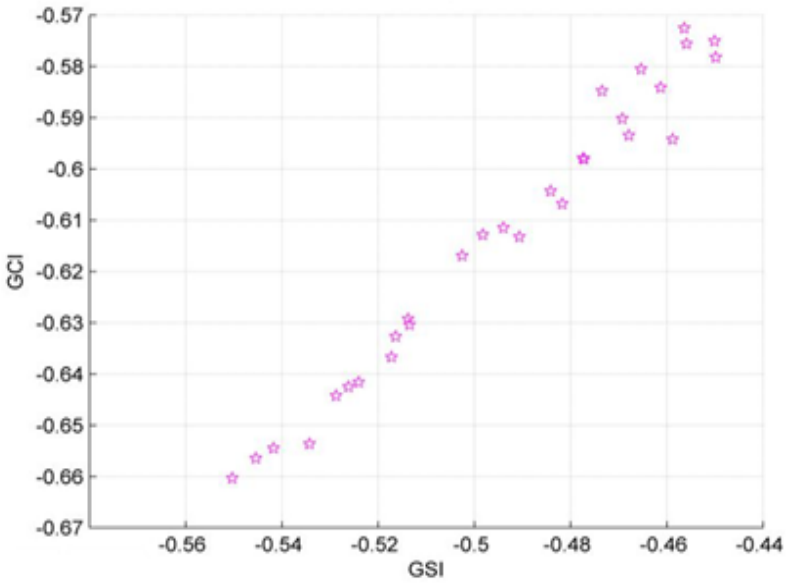


Fig. 19 Pareto optimal front for GSI vs. GSI

## IX. CONCLUSIONS

The architecture optimization for a general 3PRC parallel manipulator is carried out using CENSGA as a multi objective optimization in order to obtain large reachable workspace with improved performance having good global condition index and global stiffness index. The CENSGA is a robust optimization tool provides a final approximation set with widely spread non-dominated solutions. The described approach is absolutely generic and can be used with different objective functions and constraints. In the future work multi objective particle swarm optimization will be implemented for PKM design and the results will be compared with CENSGA.

## REFERENCES

[1] H.Kim, L. Tsai, Design optimization of a Cartesian parallel manipulator, Journal of Mechanical Design, 125(1), (2003), pp.43-52.
[2] L. Tsai, S. Joshi, Kinematics and optimization of a spatial 3-UPU parallel manipulator, Journal of Mechanical Design, (122), (2000), pp.439-446.
[3] X. Kong, C. Gosselin, Type synthesis of 3-DOF translational parallel manipulators based on screw Theory and virtual joint, in: Proceedings of 15 th CISM- IFTOMM Symposium on Robot Design, Dynamics and control (ROMANSY 2004), (126), pp.83-93.
[4] R. Di Gregorio, V. Parenti Castelli, A translational 3-DOF parallel manipulator, Advances in Robot kinematics: Analysis and Control, (3), (1998), pp.49-58.
[5] M. Callegari, M. Tarantini, Kinematic Analysis of a Novel Translational Platform, ASME J.Mech. Design, (125), (2),(2003), pp.308-315.


Published By:
Blue Eyes Intelligence Engineering
and Sciences Publication (BEIESP)

[6] Y.Li, Q.Xu, Kinematic Analysis and Design of a New 3-DOF Translational Parallel Manipulator, Journal of Mechanical Design, (128), (2006), pp.729-737.
[7] T.Huang, X. Zhao, D.J. Whitehouse, Stiffness estimation of a tripod – based parallel kinematic Machine, IEEE Trans. Robot. Automat. (18), (1), (2002), pp.50-58.
[8] M.Ceccarelli, G. Carbone, A stiffness analysis for CaPaMan (Cassino Parallel Manipulator) Mech. Mach. Theory, (37), (5),(2002),pp.427-439.
[9] Q.Xu, Y.Li, An investigation on mobility and stiffness of a 3-DOF translational parallel manipulator Via screw theory, Robotics and Computer-Integrated Manufacturing, (24), (2008), pp.402-414.
[10] X.Liu, Z.Jin, F.Gao, Optimum design of 3-dof spherical parallel manipulators with respect to the conditioning and stiffnesindices , Mechanism and Machine Theory, Vol. 35(9),(2000), pp 1257-1267.
[11] G.Alici.,B. Shirinzade, Optimum synthesis of planar parallel manipulators based on kinematic isotropy and force balancing , Robotica, Vol.22,(2004), pp. 97-108.
[12] N.M. Rao, K.M. Rao, Dimensional synthesis of a spatial 3-RPS parallel manipulator for a prescribed range of motion of spherical joints. Mechanism and Machine Theory, Vol.44,(2009), pp 477-486.
[13] F.A. Lara-Molina,J.M Rosario,D. Dumur, Multi-Objective Design of Parallel Manipulator Using Global Indices. The Open Mechanical Engineering journal, Vol.4, (2010), pp.37-47.
[14] A.M Lopes, E.J Solteiro Pires, Optimization of the Work piece Location in a Machining Robotic Cell. International journal of Advanced Robotic Systems, Vol.8 (6), (2011), pp.37-46.
[15] R. Kelaiaia, O.Company, A. Zaatric, Multiobjective optimization of a linear Delta parallel robot, Mechanism and Machine Theory, Vol.50,(2012), pp.159-178.
[16] Y.Li, Q.Xu, Stiffness analysis for a 3-PUU parallel kinematic machine, Mechanism and Machine Theory, (43), (2008), pp.186-200.
[17] C.Gosselin, Determination of the workspace of 6-DOF parallel manipulators. ASME Journal of Mechanical Design, Vol.112 (3), (1990), pp.331-337.
[18] J.P. Merlet, Determination of the orientation workspace of parallel manipulators, Journal of intelligent and robotic systems, Vol.13,(1995),pp.143-160.


*Published By:*
*Blue Eyes Intelligence Engineering and Sciences Publication (BEIESP)*